

SOME STUDIES ON THE DESATURATION AND LIQUEFACTION RESISTANCE OF AIR DESATURATED SANDY SOIL

Dhanaji CHAVAN*, Thallak SITHARAM†

Abstract: Over last few years induced desaturation of in-situ saturated sandy soils is being considered as a new liquefaction mitigation technique. In this technique, the degree of saturation of the liquefaction susceptible saturated sandy soil is reduced either by injecting air externally or generating gas in the soil matrix itself adopting techniques such as microbial denitrification. In the present study, triaxial specimens of clean sandy soils have been desaturated by two methods: CO₂ injection and air injection. It is observed that CO₂ desaturated specimen lost its desaturation over very short period of time. However, desaturation of the air injected specimens lasted for significantly long time. Further, stress controlled undrained cyclic triaxial tests have been conducted on air desaturated specimens at different relative densities, effective confining pressures and frequencies. It is observed that the number of cycles required for initial liquefaction (N_i) increases significantly on desaturation. Moreover, for a specimen of relative density (D_r) of 40 %, subjected to cyclic shear stress ratio (CSR) of 0.175 and effective confining pressure of 100 kPa, the number of cycles required for initial liquefaction (N_i) at degree of saturation (S) of 89.5 % were 18.5 times that at full saturation. A specimen with degree of saturation (S) of 81.4 % (CSR 0.175, D_r 40 %) attained a maximum pore pressure ratio of just 0.19, at the end of 350 cycles, indicating very high liquefaction resistance. Higher N_i was observed at higher frequency for a given degree of saturation (S).

Keywords: air desaturation, initial liquefaction, pore pressure ratio

Introduction

Liquefaction has been one of the main cause of devastation during earthquake events (Kramer, 1996). Failure of dams, collapse of buildings, lateral spreading, bridge failures etc. had been observed as a consequence of liquefaction of the soil. Over the period of time various liquefaction mitigation techniques such as dynamic compaction, grouting, deep mixing, blast compaction to name a few, have evolved (Idriss and Boulanger, 2008). Induced desaturation is emerging as a new liquefaction mitigation technique over last few years (Ishihara, Okamura and Oshita, 2003; Pietruszczak, Pande and Oulapour, 2003; Yegian *et al.*, 2007; He, Chu and Ivanov, 2013; He, Chu and Liu, 2014)

In the present study, triaxial specimens of clean sandy soil have been desaturated by two methods: 1) CO₂ injection 2) air injection. Further, stress controlled undrained cyclic triaxial tests have been conducted on air desaturated samples of varying degree of saturation (S) at different initial effective confining pressure and cyclic shear stress ratio (CSR).

Material

In this study, a fraction of sand passing through 2 mm Indian Standard (IS) sieve and retained on 0.075 mm IS sieve has been used. The original sand was collected from the bed of Sabarmati River near IIT Gandhinagar campus, India. As per the IS soil classification system, the sand used in this study is a poorly graded fine sand. The index properties of the sand are given in Table 1.

* Research Scholar, Dept. of Civil Engg., Indian Institute of Science, Bangalore, India,
dschavan83@gmail.com

† Professor, Dept. of Civil Engg., Indian Institute of Science, Bangalore, India,

Specific Gravity (G)	e _{max}	e _{min}	ρ _{max} (gm/cc)	ρ _{min} (gm/cc)	D ₁₀ (mm)	D ₃₀ (mm)	D ₅₀ (mm)	D ₆₀ (mm)	C _u	C _c
2.65	0.84	0.45	1.83	1.44	0.14	0.20	0.27	0.30	2.14	0.95

Table 1. Index properties of the sand used in this study

Experimental program

Sample preparation

The cylindrical specimens of size 100 mm x 50 mm (height x diameter) were prepared by dry deposition method. Mass of the sand was poured into split mold through a funnel with a spout. To begin with, the tip of the spout was placed at base of the mold and slowly raised with zero drop height. The sand was deposited in five layers and at the end of each layer, gentle tamping was done with the help of spout tip. At the end of pouring, light side taping was also done to achieve desired relative density.

Saturation

Once the sample was prepared, CO₂ gas was passed through it for 30 minutes. For first 10 minutes it was passed under vacuum of around 20 kPa and next 20 minutes under atmospheric pressure. This was followed by flushing of 1000 ml of water through the sample under very small gradient. It was observed from several trials that this combination resulted into a degree of saturation as high as 99 %. Black and Lee (1973) suggested that a sample with degree of saturation of 99 % can be considered as a saturated sample from practical point of view. Once saturation of the sample was ensured, sample was desaturated by injecting CO₂ gas/air. The desaturation procedure has been explained in detail in the following section.

Desaturation

In this study, samples have been desaturated by two methods: 1) CO₂ injection 2) air injection. Initially samples were saturated as mentioned in preceding section. After this the back pressure pipe was disconnected and CO₂/air supply pipe was connected at the bottom of triaxial cell as shown in Figure 1. Then pore pressure measuring pipe was also disconnected and a small cup to collect ejected water was placed below the drainage valve as shown in Figure 1. Then, CO₂/air was injected into the sample from bottom of the specimen under a very small pressure of around 1 kPa. As CO₂/air starts getting into the sample, it pushes out slowly some of the pore water. The pushed pore water was collected in a small cup as shown in Fig. 1. Depending upon the time for which CO₂/air was injected, different quantities of water got collected in a cup. Varying degrees of saturation were achieved by injecting CO₂/air for different time spans and pushing out different quantities of pore water. Once the desaturation was over, back pressure pipe and pore pressure measuring pipe were connected back to their pervious position. After desaturation, the degree of saturation of sample was computed as per the discussion in following section.

Computation of degree of saturation

The degree of saturation (S) of the sample has been calculated from the following equation (Lade, 2016):

$$B = \frac{1}{1 + nK_s [S/K_w + (1 - S)/u_a]} \quad (1)$$

Where, *B* is Skempton's pore pressure parameter ($\Delta u / \Delta \sigma$); *n* is porosity of the sample, *K_s* is the bulk modulus of the soil skeleton; *K_w* is the bulk modulus of the water; *u_a* is the absolute pore fluid pressure which is equal to back pressure plus Δu . To measure *B* parameter, first both back pressure and drainage valve are closed and a cell pressure increment of $\Delta \sigma$ is applied to the sample and corresponding rise in the pore water pressure Δu is noted down. The ratio of the rise in the pore water pressure (Δu) and applied cell pressure increment ($\Delta \sigma$) gives Skempton's pore pressure parameter *B*.

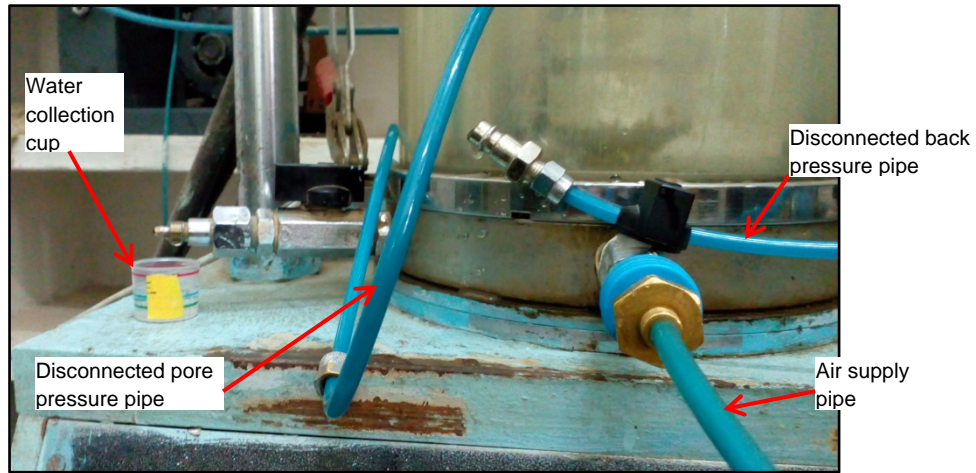


Figure 1. Connections during desaturation

It is believed that for a sample to be fully saturated the Skempton's pore pressure parameter B should be greater than 0.95 and should preferably be 1. However, from eq.1 it is clear that B parameter is dependent on not only degree of saturation but also stiffness of the soil skeleton (K_s). That is, softer is the soil skeleton, more part of the cell pressure increment $\Delta\sigma$ goes to the pore water and higher is the measured B parameter. On the other hand, stiffer is the soil skeleton, relatively less part of the cell pressure increment $\Delta\sigma$ goes to the pore water and relatively lower value of B parameter is obtained. Moreover, B parameter of 1 is possible only when all applied cell pressure increment goes to the pore water. This is possible only when the stiffness of the soil skeleton is zero. This reasoning is well supported by eq.1 as well. We get, B as 1 only when value of K_s is zero in this equation.

Plot of B parameter versus degree of saturation (S) obtained from eq.1 is shown in Fig. 2. This plot is obtained for a sample of relative density (D_r) of 40 % having K_s 1.03×10^4 kPa and n 0.406. The bulk modulus of water is 2.23×10^6 kPa. The back pressure in this case is atmospheric pressure. From Fig. 2 it is clear that a B parameter of even 0.7 results into a degree of saturation as high as 98.3 % and a B parameter of 0.8 results into a degree of saturation of 99 %. Moreover, increase in B parameter from 0.80 to 0.99 results into increase in S just from 99 % to 99.99 %. In this study, samples with S of 99 % has been treated as saturated samples. The B parameter for these samples was around 0.8.

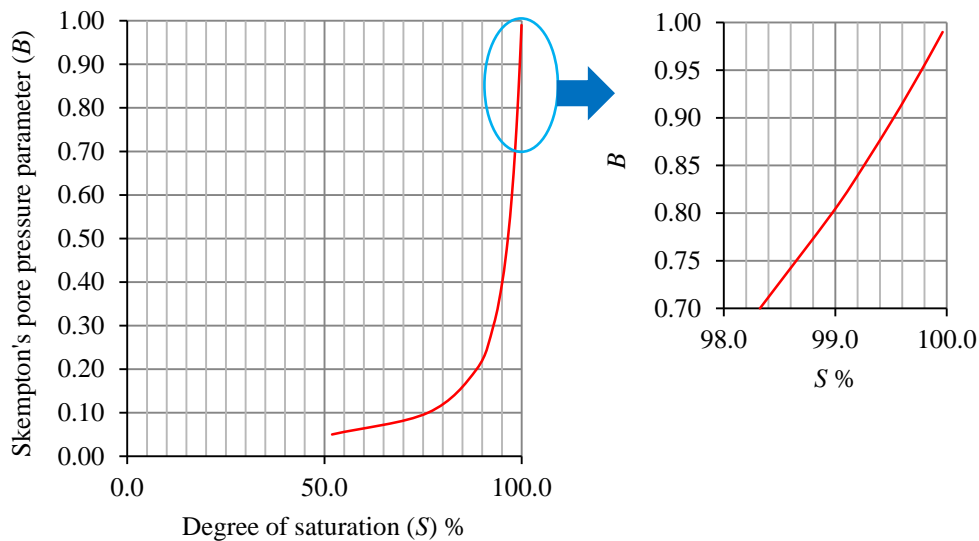


Figure 2. Variation of B parameter with degree of saturation (S)

CO₂ desaturation versus air desaturation

To begin with, about 30 samples were desaturated by injecting CO₂ gas into the sample. However, consistency in the observed results was missing. The source of doubt was possible alteration of degree of saturation of the sample over the period of time. To confirm this, later on longevity of injected CO₂ gas was checked. It was found that injected CO₂ gas lasted for very short period of time owing to its dissolution into pore water. The procedure adopted in assessing longevity of injected CO₂ gas is briefed below:

First of all sample was desaturated as mentioned earlier. Then back pressure valve was closed and a cell pressure increment of 20 kPa was applied to the sample. Depending upon the degree of saturation, part of this pressure was transferred to the pore water and a sudden rise in the pore water pressure (Δu) was observed. Then, this rise in the pore water pressure was monitored for a period of time. It was observed that with the passage of time there was gradual reduction in the Δu as seen Fig. 3a. After several minutes Δu became zero. This happened due to dissolution of injected CO₂ gas into pore water.

It is a well-known fact that air has very low solubility in water. Therefore, in next attempt samples were desaturated by air. Here also longevity of injected air was assessed. It was observed that injected air lasted for long time as shown in Fig. 3b.

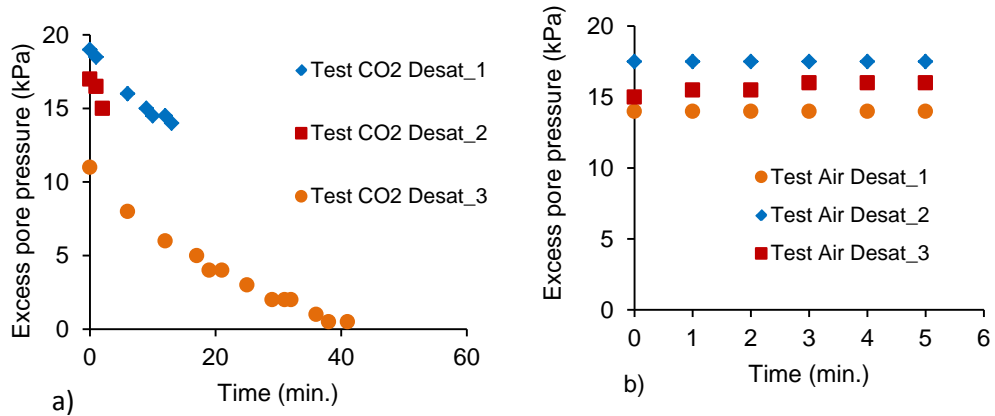


Figure 3. Assessment of longevity of desaturation: a) CO₂ desaturation b) air desaturation

Response of saturated and desaturated samples

Stress controlled undrained cyclic triaxial tests have been conducted on both saturated and air desaturated samples of relative density (D_r) of 40 % and 60 %. The samples were subjected to sinusoidal loading of frequency of 0.1 Hz, unless otherwise specified, and cyclic shear stress ratio of (CSR) 0.175 and 0.250. Samples with varying degrees of saturation were obtained by injecting air from bottom of the sample and ejecting different quantities of pore water from top. The degree of saturation of these samples was calculated from eq. 1. More was the quantity of ejected water, lower was the degree of saturation. The quantity of water ejected and corresponding degree of saturation are given in Table 2 for some of the samples. From Table 2 it is observed that degree of saturation of 94 % was achieved by ejecting 5.0 ml and 3.0 ml of water from samples of D_r 40 % and 60 %, respectively.

Relative density %	Volume of water ejected (ml)	B parameter	Degree of saturation %
40	2.5	0.50	96.6
	5.0	0.34	94.1
	7.0	0.24	91.0
60	3.0	0.35	94.0
	5.0	0.27	91.9
	10	0.13	82.1

Table 2. Degree of saturation at various water volume ejections

Thus, same degree of saturation was achieved by ejecting different quantities of water. This is so because void space available in sample of D_r 40 % is less than that in D_r 60 %. Therefore, relatively less quantity of water needs to be ejected from sample of D_r 60 % to achieve the same degree of saturation which is achieved in D_r 40 % sample.

Response of saturated sample (S 99 %) and air desaturated sample with S 89.5%, of D_r 40 %, subjected to CSR of 0.175 at initial effective confining pressure of 100 kPa is shown in Fig. 4. The response comprises evolution of pore pressure ratio (r_u), evolution of axial strain, stress strain curve and effective stress path. In Fig. 4, σ_d is deviatoric stress and σ'_c is initial effective confining pressure. In this figure, effective mean stress is calculated as $(2\sigma'_c + \sigma'_1)/3$, where σ'_1 is the effective axial stress. Further, pore pressure ratio (r_u) is the ratio of excess pore water pressure and initial effective confining pressure. From this figure it is clear that in case of saturated sample, pore pressure ratio becomes 1 at the end of 6th cycle whereas in case of S 89.5 % it becomes 1 at the end of 111th cycle. The state of attaining r_u of 1 is called as initial liquefaction. Thus, the liquefaction resistance, measured in terms of number of cycles required for initial liquefaction (N_i), of sample with S 89.5 % is 18.5 times higher than that of S 99 %. This increase in liquefaction resistance is attributed to presence of injected air in the voids of the sample. Due to air, pore fluid becomes highly compressible. This compressibility of the pore fluid delays the generation of high pore pressure, as shown in Fig. 4b, which in turn delays occurrence of the initial liquefaction. From the axial strain evolution plots it is clear that for first few cycles sample undergoes very small compression. However, after reaching certain limiting high pore pressure it undergoes both compression as well as extension. The stress strain curve shows sharp peaks on both side of vertical axis followed by large axial straining. This type of response is called as cyclic mobility wherein sample undergoes large but limited axial straining even after reaching a state of zero deviatoric stress. From the effective stress path it is observed that effective mean stress gradually decreases with loading and eventually becomes zero. Once the effective mean stress becomes zero, the stress path emanates from origin over consecutive loading-unloading cycles. Similar kind of response was observed for saturated and desaturated samples of D_r 60 % as well but for brevity not shown here. In case of D_r 60 %, tests were conducted at CSR of 0.250 and initial effective confining pressure of 100 kPa.

Response of a sample of D_r 40 % at low degree of saturation i.e., S 81.4 % and at CSR of 0.175 and initial effective confining pressure of 100 kPa is shown in Fig. 5. From this figure it is clear that sample does not undergo initial liquefaction even at the end of 350 cycles. The maximum pore pressure ratio attained in this case was just 0.19. This indicates extremely high liquefaction resistance of sample at low degree of saturation.

Degree of saturation versus N_i

As discussed in the previous section, liquefaction resistance, measured in terms of N_i , increases on desaturation. To understand the relationship between the two, degree of saturation is plotted against N_i , as shown in Fig. 6, for D_r 40 % and 60 %. From Fig. 6 it is observed that the liquefaction resistance increases exponentially with reduction in the degree of saturation, for both relative densities. Few tests were conducted on samples of D_r 40 % at initial effective confining pressure of 50 kPa and CSR 0.250. In this case also N_i increased exponentially with decrease in S.

Effect of frequency on liquefaction resistance

Few tests were conducted to study the effect frequency of loading on the liquefaction resistance of desaturated samples. Plots of degree of saturation versus N_i at frequency of 0.1 Hz and 0.2 Hz are shown in Fig. 7. For both frequencies the liquefaction resistance increases exponentially with decrease in degree of saturation. Further, it is observed that for saturated/nearly saturated samples effect of frequency is negligible on liquefaction resistance. However, as the degree of saturation decreases the frequency effect becomes predominant. For sample with S 81.5 %, N_i at frequency of 0.2 Hz is 1.8 times higher than that at frequency of 0.1 Hz. Thus, liquefaction resistance of desaturated samples is frequency dependent. On the other hand, liquefaction resistance of saturated/nearly saturated samples is frequency independent.

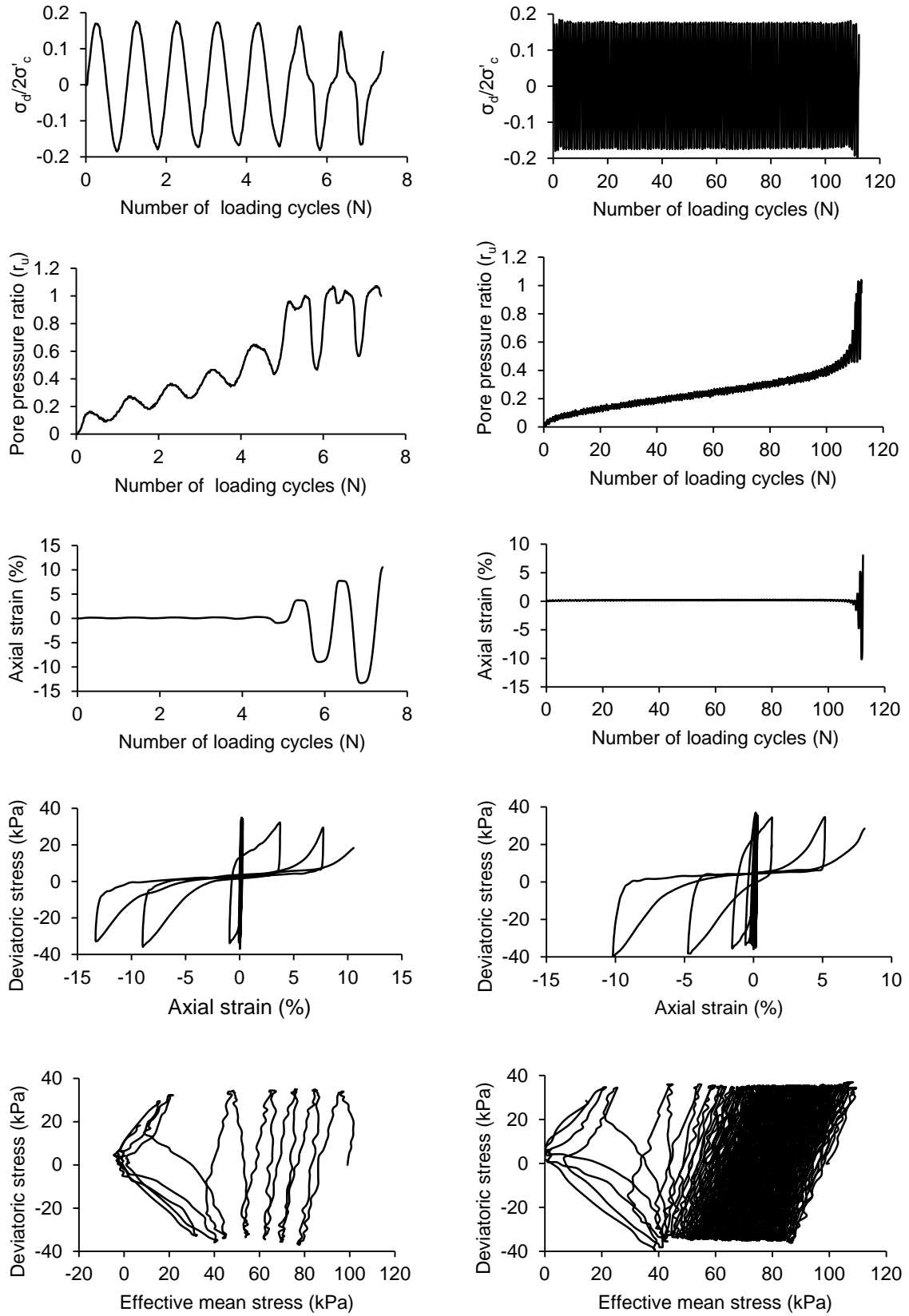


Figure 4. Response of saturated and desaturated samples of $D_r 40\%$ at $CSR 0.175$ and $\sigma'_c 100 \text{ kPa}$: a) S 99 % b) S 89.5 %

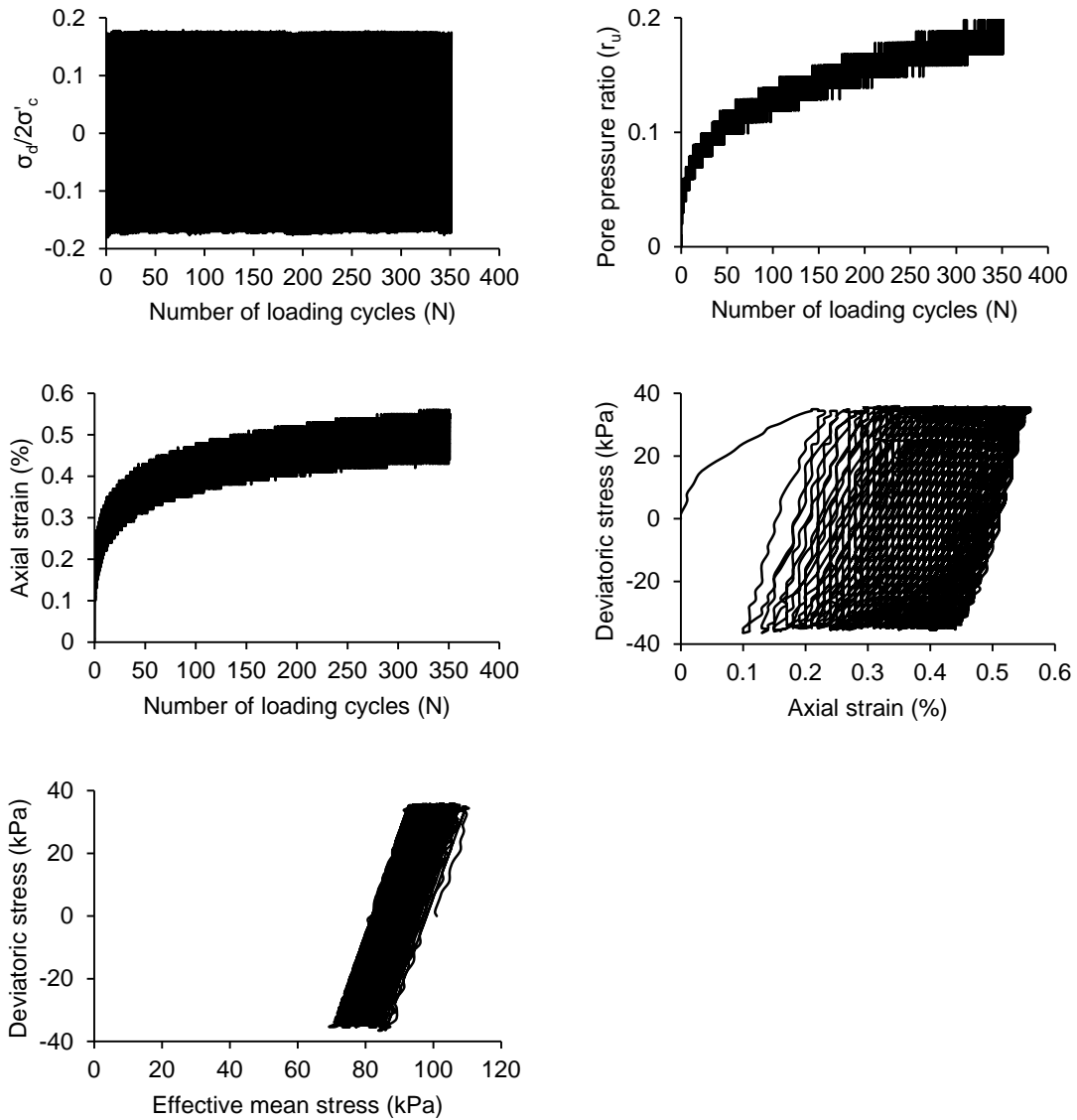


Figure 5. Response of desaturated sample (S 81.4 %) of D_r 40 % at CSR 0.175 and σ'_c 100 kPa

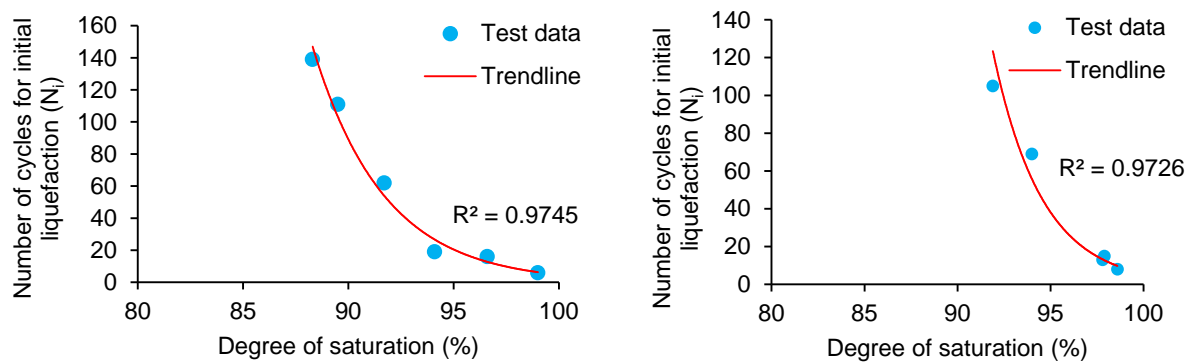


Figure 6. Degree of saturation versus N_i for: a) D_r 40 %, CSR 0.175 and σ'_c 100 kPa b) D_r 60 %, CSR 0.250 and σ'_c 100 kPa

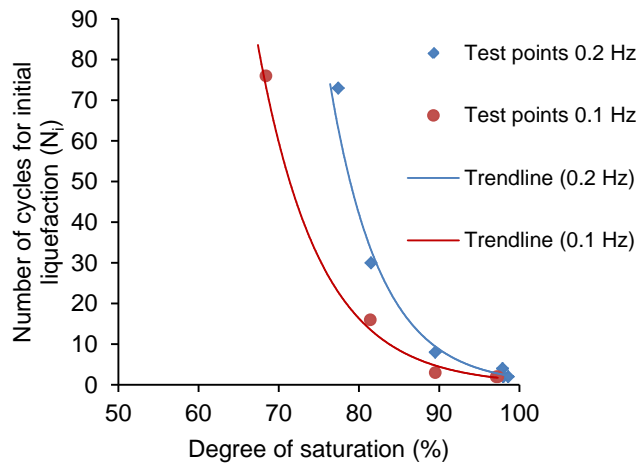


Figure 7. Effect of frequency on N_i of air desaturated samples

Conclusions

From the present study it is found that CO_2 desaturation is lost over very short period of time. On the other hand, air desaturation lasts for very long time owing to significantly low solubility of air in pore water. Liquefaction resistance of the sample is found to increase on desaturation. Further, there is exponential increase in the liquefaction resistance with decrease in the degree of saturation. It is observed that liquefaction resistance of saturated/nearly saturated sample is frequency independent. However, liquefaction resistance of desaturated samples is highly frequency dependent. Lower is the degree of saturation more predominant is the frequency effect on liquefaction resistance.

References

- Black, D. and Lee, K. (1973) 'Saturating laboratory samples by back pressure', *Journal of Soil Mechanics & Foundations Div*, 99(SM1), pp. 75–95.
- He, J., Chu, J. and Ivanov, V. (2013) 'Mitigation of liquefaction of saturated sand using biogas', *Géotechnique*, 63(4), pp. 267–275. doi: 10.1680/geot.SIP13.P.004.
- He, J., Chu, J. and Liu, H. (2014) 'Undrained shear strength of desaturated loose sand under monotonic shearing', *Soils and Foundations*, 54(4), pp. 910–916.
- Idriss, I. M. and Boulanger, R. . (2008) *Soil liquefaction during earthquakes*. EERI.
- Ishihara, M., Okamura, M. and Oshita, T. (2003) 'Desaturating sand deposit by air injection for reducing liquefaction potential', *Pacific Conference on Earthquake Engineering*, (89).
- Kramer, S. L. (1996) *Geotechnical Earthquake Engineering*. PEARSON.
- Lade, P. V (2016) *Triaxial Testing of Soils*. First edit. John Wiley & Sons, Ltd.
- Pietruszczak, S., Pande, G. N. and Oulapour, M. (2003) 'A hypothesis for mitigation of risk of liquefaction', *Géotechnique*, 53(9), pp. 833–838. doi: 10.1680/geot.2003.53.9.833.
- Yegian, M. K., Eseller-Bayat, E., Alshawabkeh, A. and Ali, S. (2007) 'Induced-partial saturation for liquefaction mitigation: experimental investigation', *Journal of Geotechnical and Geoenvironmental Engineering*, 133(4), pp. 372–380. doi: 10.1061/(ASCE)1090-0241(2007)133:4(372).